



# Synchronization transitions on complex thermo-sensitive neuron networks with time delays

Yanhang Xie, Yubing Gong\*, Yinghang Hao, Xiaoguang Ma

School of Physics, Ludong University, Yantai, Shandong 264025, PR China

## ARTICLE INFO

### Article history:

Received 29 October 2009

Received in revised form 16 November 2009

Accepted 16 November 2009

Available online 30 November 2009

### Keywords:

Thermo-sensitive neuron network

Time delay

Synchronization transition

Stochastic dynamics

## ABSTRACT

We have numerically studied the firing synchronization transitions on random thermo-sensitive neuron networks in dependence on information transmission delay  $\tau$ , network randomness  $p$ , and coupling strength  $g$ . It is found that as  $\tau$  is increased the neurons can exhibit transitions from burst synchronization (BS) to clustering anti-phase synchronization (APS), and further to spike synchronization (SS). It is also found that, with increasing  $p$  or  $g$ , there are transitions from spatiotemporal chaos to BS, then to APS, and finally to SS. However, the APS state with  $p$  or  $g$  exists only for intermediate  $\tau$  values within a narrow range. For  $\tau$  values outside this range, the APS state does not appear and the firings change directly from spatiotemporal chaos to BS or SS. These results show that, as time delay can do, network topology and coupling strength can also cause complex synchronization transitions in the neurons. In particular, the novel phenomenon of APS state with  $p$  or  $g$  shows that, with the help of appropriate random connections or coupling strength, the neurons may exhibit the APS behavior at a certain time delay for which the APS does not appear originally. These findings imply that time delay, network randomness, and coupling strength may have subtle effects on the firing behaviors on neuronal networks, and thus could play important roles in the information processing in neural systems.

© 2009 Elsevier B.V. All rights reserved.

## 1. Introduction

In the last three decades, the constructive roles of noise have been extensively studied in different nonlinear dynamical systems [1]. Neurons are noisy elements. Noise arises from both external (e.g., synapses) and internal (e.g., channels) sources. The effects of external and internal noise in the firing dynamics of neurons have been extensively studied [2–15]. On the other hand, since the information processing and signal transduction in neurons is fulfilled via coupled neurons and uncertainty due to stochasticity in biophysical processes exists in the communication between the neurons, firing dynamics of random complex neuron networks has received considerable attention [16–20].

Synchronization phenomena are ubiquitous in nature and play important roles in various fields such as physics, chemistry, ecology, and biology. In neuronal systems, synchronous activity is considered to play important roles in information processing in the brain [21–23], but they are not desirable for several neurological diseases such as epilepsy and tremor in Parkinson's disease [24,25]. In recent years, people have performed extensive study on the firing dynamics of neuronal systems [26] and found many synchronization phenomena [27–41], such as

noise-induced synchronization in modified Hodgkin–Huxley neurons (MHH) [29], chemical synapse-induced bursting synchronization in a ring neuronal network [30] and two coupled map-based neurons [31], synchronization in a square lattice noisy neuronal network [32], maximal spatial synchronization on scale-free networks of Morris–Lecar neurons at optimal noise intensity and coupling strength [33], burst-enhanced synchronization in an array of noisy coupled MHH neurons [34], synchronization in a large ensemble of MHH neurons with gap junctions [35], and synchronization on small-world networks of neurons [17,36–39]. Recently, transitions of firing behaviors in neuronal systems have attracted growing attention, and the transition from spatiotemporal chaos to bursting synchronization (BS) with increasing coupling strength in Hindmarsh–Rose neuron networks [40] and the transitions between various synchronization states under different coupling strengths and external currents in two electrically-coupled MHH neurons [41] have been observed.

In neuronal systems, time delays are inherent because of both finite propagation velocities in the conduction of signals along neurites and delays in the synaptic transmission [42]. In recent years, the effects of time delay on the firing dynamics of neuronal systems have been intensively studied. People have found that time delays can facilitate and improve neuronal synchronization [43–45], destabilize synchronous states and induce near-regular wave states [46], induce various spatiotemporal patterns [47] and multiple stochastic resonances [48], and enhance the coherence of spiral waves [49]. In addition, time delays have subtle roles in the synchronization transitions on neuronal networks. It is found that

\* Corresponding author. Tel.: +86 535 6697550.

E-mail address: [gongyubing09@hotmail.com](mailto:gongyubing09@hotmail.com) (Y. Gong).

time delays can induce the transitions between in-phase and anti-phase synchronizations in two coupled fast-spiking neurons [50], the transitions from zigzag fronts to clustering anti-phase synchronization and further to regular in-phase synchronization on small-world neuronal networks of the Rulkov map [51], and can intermittently induce the synchronization transitions on scale-free neuronal networks [52].

In this paper, we study the effect of time delay  $\tau$ , topological randomness  $p$ , and coupling strength  $g$  in the wave formation and spatial synchronization in noisy chaotic MHH neuron networks. Complex synchronization transition with changing  $\tau$ ,  $p$  or  $g$  has been found. In particular, anti-phase synchronization has been observed in the transitions with changing  $p$  or  $g$ . This result reveals novel significance of  $p$  and  $g$  for the firing behaviors in the neurons.

## 2. Model and equations

The MHH model was proposed by Braun et al. [53] and has been used for describing thermo-sensitive neurons. The model can produce fruitful firing patterns that can be observed in electro-receptors like dogfish [54], catfish [55], and facial cold receptors of rat [56]. These neurons can be characterized by spontaneous and noisy oscillations that are reflected in spike or burst trains.

The random neuronal network herein is constructed as follows [17,37]: We start with a one-dimensional regular chain which comprises  $N=60$  identical chaotic MHH neurons with each one being connected to its two nearest neighbors. Links are then randomly added between non-nearest vertices. In the limit case, all neurons are coupled to each other and the network contains  $N(N-1)/2$  edges. Using  $M$  to denote the number of added shortcuts, hence the fraction of the shortcuts is given by  $p = M/[N(N-1)/2]$ , which can be used to characterize the randomness of the network. In Fig. 1, the schematic presentations of the networks with  $p=0$  and  $p=0.11$  are displayed. Please note that for a given  $p$  there are a lot of network realizations.

In the presence of time delay, the membrane potential of each neuron in the coupled neurons is given by

$$C_M \frac{dV_i}{dt} = -I_{iNa} - I_{iK} - I_{isd} - I_{isa} - I_{il} + \sum_j g_{ij} [V_j(t-\tau) - V_i] + D\xi_i(t), \quad (1)$$

where  $C_M$  is the membrane capacitance,  $\xi_i(t)$  denotes the noise in each neuron, and  $\sum_j g_{ij} [V_j(t-\tau) - V_i]$  represents the coupling between two neurons. The currents consist of five terms and fall into three groups. The first two,  $I_{iNa}$  and  $I_{iK}$ , are the fast sodium and potassium currents that generate the action potentials,

$$I_{iNa} = \rho g_{Na} a_{Na} (V_i - V_{Na}), \quad (2)$$

$$I_{iK} = \rho g_K a_K (V_i - V_K), \quad (3)$$

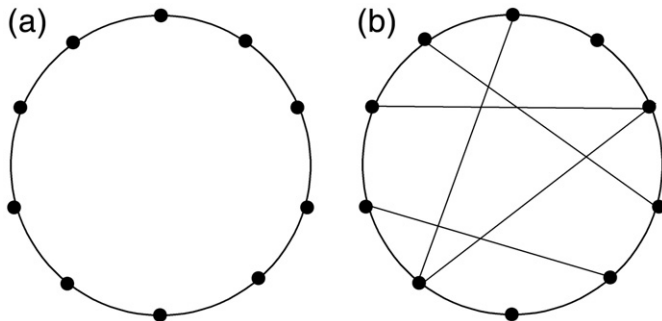


Fig. 1. Schematic presentation of the network with  $N=10$  neurons. (a) Regular ring ( $p=0$ ). (b) Random network ( $p \approx 0.11$ ).

where the  $g$ 's are the conductances and the  $a$ 's contain the switching characteristics of the channels. In the steady state

$$a_{Na,\infty} = a_{K,\infty} = \frac{1}{1 + \exp[-0.25(V_i + 25)]}. \quad (4)$$

The sodium and potassium currents relax exponentially

$$\frac{da_{Na}}{dt} = \frac{\phi}{\tau_{Na}} (a_{Na,\infty} - a_{Na}), \quad (5)$$

$$\frac{da_K}{dt} = \frac{\phi}{\tau_K} (a_{K,\infty} - a_K). \quad (6)$$

The dimensionless factors  $\rho$  and  $\phi$  contain the temperature dependence

$$\rho = 1.3^{(T-T_0)/10}, \quad (7)$$

$$\phi = 3.0^{(T-T_0)/10}, \quad (8)$$

where the reference temperature is  $T_0 = 25^\circ\text{C}$ . The next two currents in Eq. (1) describe the slow currents that are given by

$$I_{isd} = \rho g_{sd} a_{sd} (V_i - V_{sd}), \quad (9)$$

$$I_{isa} = \rho g_{sa} a_{sa} (V_i - V_{sa}), \quad (10)$$

where the indices sd and sa stand for “slow depolarization” and “slow after hyperpolarization.” They are resumed to relax according to

$$\frac{da_{sd}}{dt} = \frac{\phi}{\tau_{sd}} (a_{sd,\infty} - a_{sd}), \quad (11)$$

$$\frac{da_{sa}}{dt} = \frac{\phi}{\tau_{sa}} (-\eta I_{isd} - k a_{sa}), \quad (12)$$

where  $\eta = 0.012 \mu\text{A}$ ,  $k = 0.17$ , and

$$a_{sd,\infty} = \frac{1}{1 + \exp[-0.09(V_i + 40)]}. \quad (13)$$

The temperature dependence is controlled by the same factors  $\rho$  and  $\phi$  as above. Finally, the leak current  $I_{il}$  is given as

$$I_{il} = g_l (V_i - V_l). \quad (14)$$

The values of parameters that appear in the above equations are listed in Table 1.

In the coupling term  $\sum_j g_{ij} [V_j(t-\tau) - V_i]$ ,  $V_i$  is the membrane potential of the  $i$ -th neuron at time  $t$ ,  $V_j(t-\tau)$  is the membrane potential of the  $j$ -th neuron at earlier time  $t-\tau$ , where  $\tau$  is the time delay;  $1 \leq (ij) \leq N$ , and the summation takes over all neurons;  $g_{ij}$  is a coupling constant between the two neurons  $i$  and  $j$ , which is

Table 1  
Values of parameters used in the model.

Membrane capacitance $C_M = 1 \mu\text{F}/\text{cm}^2$	
Conductances ( $\text{mS}/\text{cm}^2$ )	
$g_{Na} = 1.5$	$g_K = 2.0$
$g_{sd} = 0.25$	$g_{sa} = 0.4$
$g_l = 0.1$	
Time constants (ms)	
$\tau_{Na} = 0.05$	$\tau_K = 2.0$
$\tau_{sd} = 10$	$\tau_{sa} = 20$
Reversal potentials (mV)	
$V_{Na} = V_{sd} = 50$	$V_K = V_{sa} = -90$
$V_l = -60$	

determined by the coupling pattern of the system and is identical for any two neurons, i.e.,  $g_{ij}=g$ . If neurons  $i$  and  $j$  are connected, they have a constant coupling strength  $g$ ; otherwise  $g=0$ .

The MHH neuron model is temperature-dependent and can exhibit distinct dynamical behaviors with the change of the temperature. It behaves like regular spikes ( $T < 7.31^\circ\text{C}$ ), chaotic bursts ( $7.31^\circ\text{C} \leq T \leq 10^\circ\text{C}$ ), and regular bursts ( $T > 10^\circ\text{C}$ ) [57]. To study the effects of time delay, topological randomness, and coupling strength on wave formation and spatial synchronization for chaotic firings on the neuronal networks, we fix the temperature  $T = 8.2^\circ\text{C}$ , such that the system is located in a chaotic region and hence each neuron fires chaotic bursts. Noises  $\xi_i(t)$  are Gaussian white ones with  $\langle \xi_i(t) \rangle = 0$  and  $\langle \xi_i(t)\xi_j(t') \rangle = D\delta_{ij}\delta(t-t')$ , where  $D$  is the noise intensity.

Numerical integration of Eq. (1) is carried out by using the explicit Euler method with time step 0.01 ms. Periodic boundary conditions are employed and the parameter values for all the neurons are identical except for distinct initial values of potential  $V_{i0}$  and the noise terms  $\xi_i(t)$  for each neuron.

### 3. Result and discussion

Firstly, we investigate how the time delay  $\tau$  affects the firing behavior. The noise intensity is fixed at  $D = 0.01$  throughout this paper. We fix the coupling strength  $g = 0.02$ . For each  $\tau$ , the average over 50 calculations (i.e., 50 realizations of networks) is performed, and in each calculation the initial values of 60 neurons' membrane potentials are chosen randomly. Fig. 2 displays the spatiotemporal evolution for different values of  $\tau$  at  $p = 0.2$ . In the absence of time delay, i.e.,  $\tau = 0$ , all the neurons exhibit BS behavior; with increasing  $\tau$ , the BS begins to be deteriorated (e.g.,  $\tau = 20$ ); when  $\tau$  is increased to  $\tau = 25$ , alternative layer waves are present and excitatory spikes alternatively appear among nearby clusters in space as the temporal dynamics evolves; as  $\tau$  is further increased, SS patterns appear (e.g.,  $\tau = 100$ ). The local enlargement for  $\tau = 25$  in Fig. 2 is displayed in

Fig. 3(a), where the APS clearly appears among the nearby clusters. For a clearer presentation of this phenomenon, the time series of two nearest neurons (e.g.,  $i = 24$  and  $j = 25$ ) is also plotted in Fig. 3(b), where synchronization transitions from BS to APS and further to SS are clearly shown (from top to bottom). The transition from BS to SS shows that more spikes are fired and, accordingly, the firing frequency is increased. This phenomenon can be explained by the mechanism that the time delay can introduce phase slips, and hence zigzag fronts as well as alternative layer waves can appear.

To quantitatively characterize the behavior, we introduce the standard deviation  $\sigma$  to measure the degree of spatial synchronization, which is defined as

$$\sigma = [\langle \sigma(t) \rangle], \quad (15)$$

with

$$\sigma(t) = \sqrt{\left[ \frac{1}{N} \sum_{i=1}^N V_i(t)^2 - \left( \frac{1}{N} \sum_{i=1}^N V_i(t) \right)^2 \right] / (N-1)}, \quad (16)$$

where  $\langle \cdot \rangle$  denotes the average over time and  $[\cdot]$  the average over 50 different network realizations for each  $p$ . The value of  $\sigma(t)$  measures the spatial synchronization of the neurons' spikes at a fixed time  $t$ . Smaller  $\sigma$  denotes more synchronization of the firings in the neurons.

The standard deviation  $\sigma$  vs.  $\tau$  for different  $p$  at  $g = 0.02$  is displayed in Fig. 4. It is seen that as  $\tau$  is increased,  $\sigma$  initially increases, then passes through a maximum, and finally monotonously decreases, which implies that BS is deteriorated first, then APS occurs, and finally the neurons exhibit SS behavior. For larger  $p$ , the  $\tau$  value where the peak for APS shifts to smaller, which shows that the more complex the network is, the shorter is the time delay for inducing the occurrence of APS.

In Fig. 5 we plot  $\sigma$  vs.  $\tau$  for different  $g$  at  $p = 0.1$ . It is seen that for each  $g$ ,  $\sigma$  first increases, then passes through a maximum, and finally

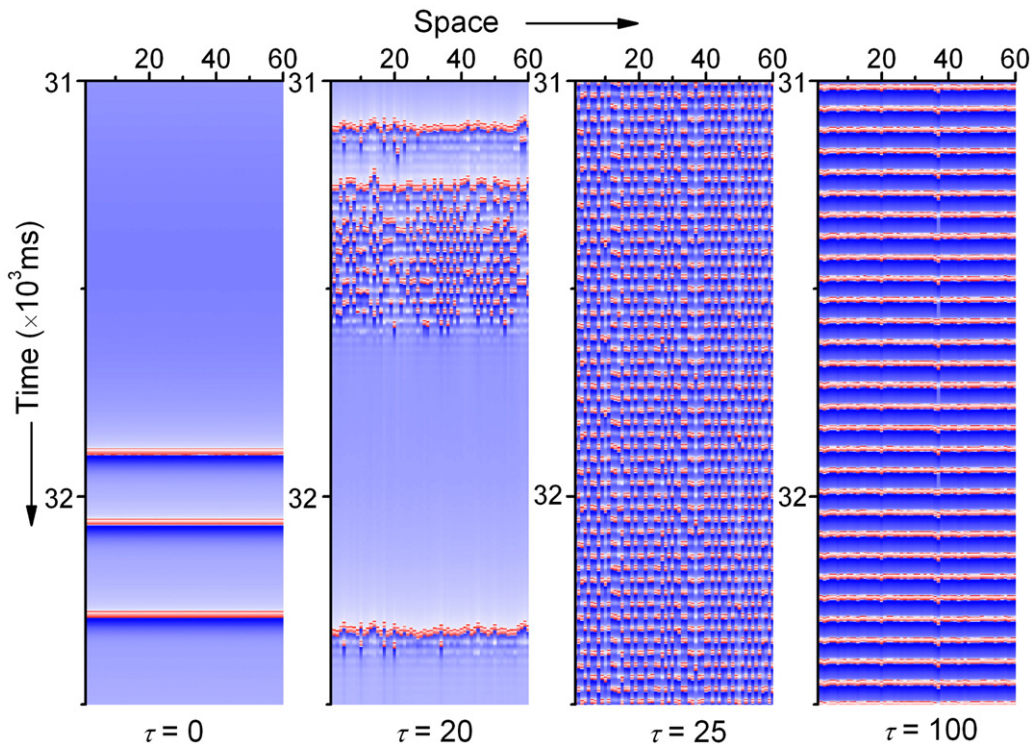
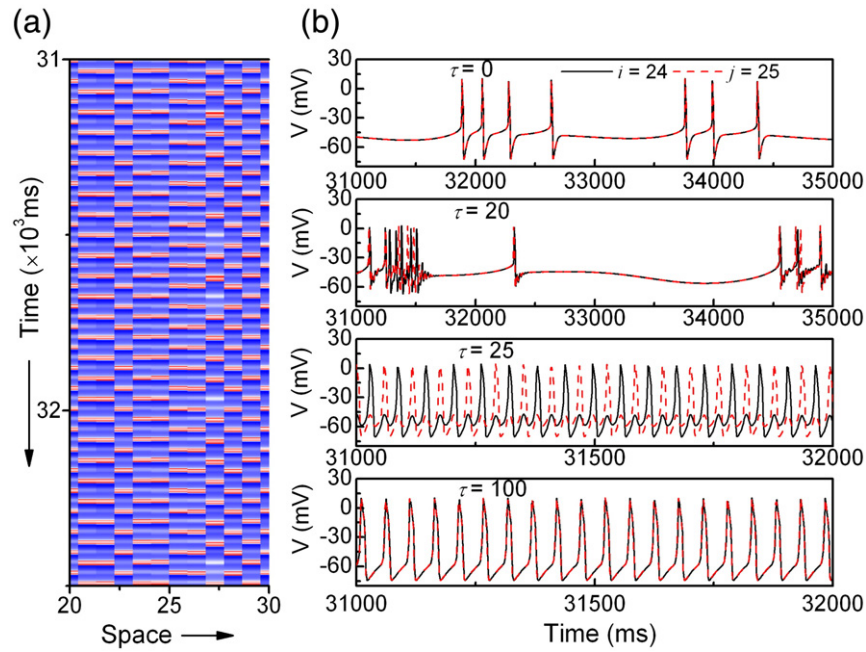


Fig. 2. Spatiotemporal evolution of membrane potentials of 60 coupled neurons on networks for different  $\tau$  when  $g = 0.02$  and  $p = 0.2$ . Synchronization transitions from BS to APS and further to SS are observed. In all panels, the abscissa represents the neurons and the ordinate represents the time changing from top to bottom. The bright regions show the firing, while the dark ones show the quiescence of neurons.



**Fig. 3.** (a) Inset for  $\tau = 25$  in Fig. 2. It clearly shows cluster anti-phase synchronization. (b) Time series of membrane potentials of two nearest neurons ( $i = 24$  and  $j = 25$ ), where APS state can be clearly observed at  $\tau = 25$ . Note that time scales in panel (b) are different.

monotonously decreases with increasing  $\tau$ , which indicates the deterioration of BS, then the transition from BS to APS and finally to SS. For a larger  $g$ , the  $\tau$  value where the APS occurs shifts to smaller, which means that the stronger the coupling is, the shorter is the time delay for inducing APS. From Figs. 4 and 5 one can see that the network randomness  $p$  and the coupling strength  $g$  have the same effects for the synchronization transitions as the time delay  $\tau$ .

Secondly, we investigate the effect of network randomness  $p$ . The firing patterns for  $p = 0, 0.15, 0.33$ , and  $0.7$  at  $g = 0.02$  and  $\tau = 20$  are displayed in Fig. 6, where four different types of firing patterns are clearly presented. At  $p = 0$  (regular ring) the firings are chaotic. As  $p$  is increased to  $p = 0.15$  the neurons display BS pattern, and for larger  $p$  to  $p = 0.33$ , the APS state is reached. However, as  $p$  is further increased, e.g.,  $p = 0.7$ , the firings turn into SS. Fig. 7 plots the evolution of  $\sigma$  as a function of  $p$  for different  $\tau$  at  $g = 0.02$ . It is seen that as  $p$  is increased,  $\sigma$  first passes through a minimum, then

increases and goes through a peak, and finally decreases monotonously, which indicates the transitions from spatiotemporal chaos to BS at first, then to APS, and finally to SS. This evolution quantitatively characterizes the synchronization transitions with changing network randomness  $p$ . For larger  $\tau$ , the  $p$  values for BS and APS shift to smaller, indicating that when time delay is longer, BS and APS will occur at a simpler network structure. However, these transitions only occur within a narrow interval of  $\tau = 20$ – $50$ . When  $\tau$  value is out of this range (e.g.,  $\tau = 10$  and  $\tau = 100$ )  $\sigma$  decreases monotonously with increasing  $p$ , indicating that there is no APS appearing. Detailed investigations showed that the firings turn directly from spatiotemporal chaos to BS (e.g.,  $\tau = 10$ ) or to SS (e.g.,  $\tau = 100$ ) (not shown). This result means that the occurrence of APS with changing  $p$  strongly depends on the value of time delay  $\tau$ . The novel phenomenon of the occurrence of APS with changing  $p$  shows that the appropriate network randomness  $p$  can also evoke the APS in firings of the neurons, as the time delay does.

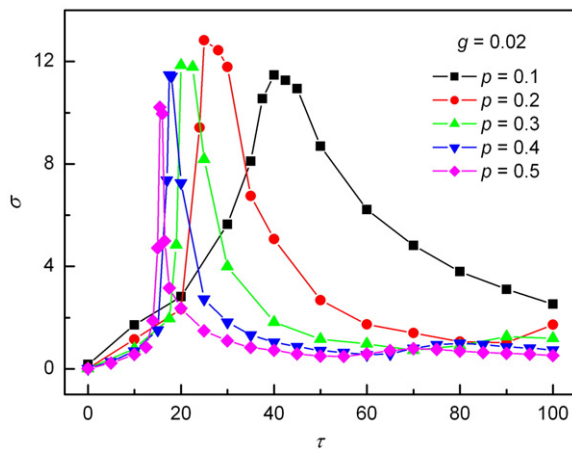


**Fig. 4.** Dependence of  $\sigma$  on  $\tau$  for different  $p$  at  $g = 0.02$ . For each  $p$ ,  $\sigma$  initially increases and passes through a peak, and then monotonously decreases with increasing  $\tau$ , characterizing the transitions from BS to APS and then to SS. For larger  $p$ , the  $\tau$  value where the APS occurs shifts to smaller.

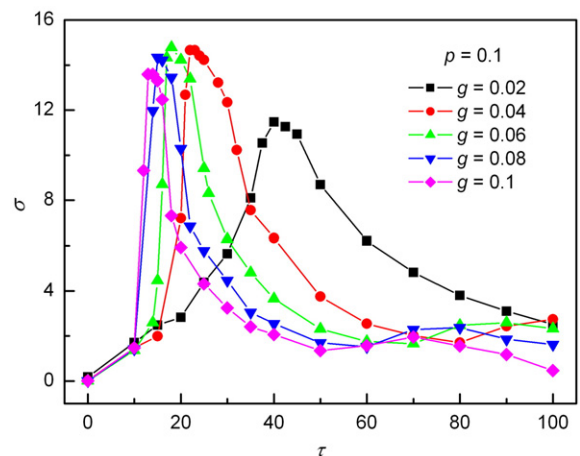


**Fig. 5.** Dependence of  $\sigma$  on  $\tau$  for different  $g$  at  $p = 0.1$ . The evolution of  $\sigma$  with increasing  $\tau$  for different  $g$  is similar to that for different  $p$  in Fig. 4.



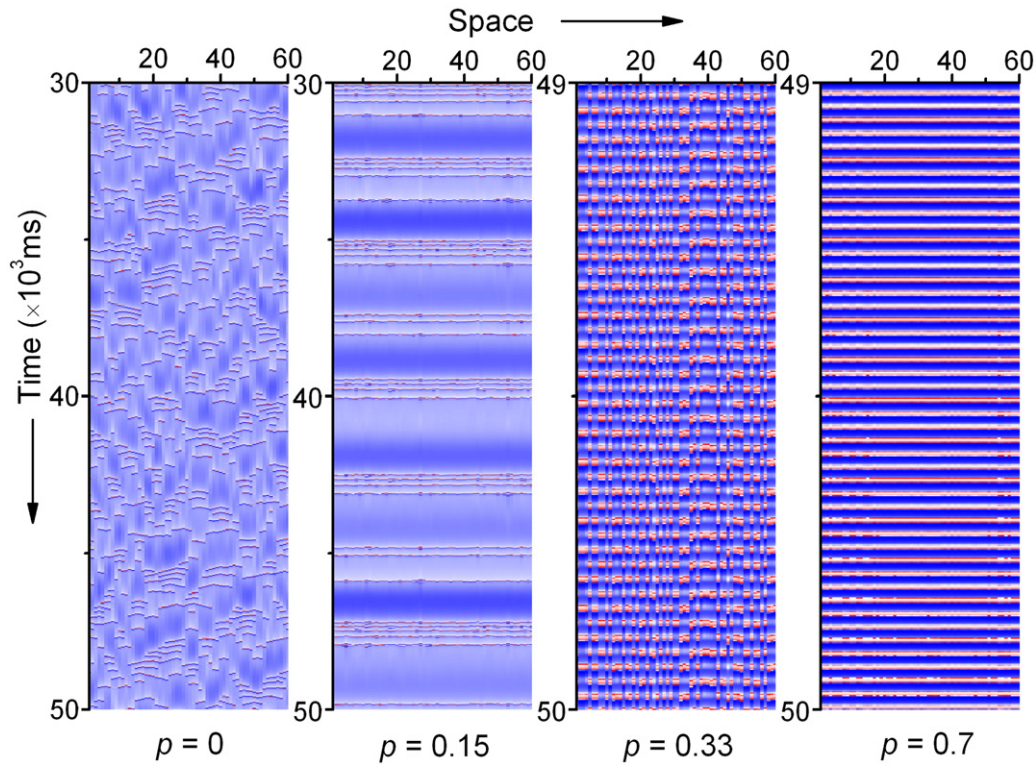


**Fig. 6.** Spatiotemporal evolution of membrane potentials for  $p = 0, 0.15, 0.33$ , and  $0.7$  at  $g = 0.02$  and  $\tau = 20$ . As  $p$  is increased, the neurons exhibit transitions from spatiotemporal chaos to BS, then to APS, and finally to SS.

Finally, we inspect the impact of coupling strength  $g$ . The spatiotemporal patterns for  $g = 0, 0.04, 0.08$ , and  $0.2$  at  $p = 0.1$  and  $\tau = 15$  are presented in Fig. 8. It is seen that the synchronization transitions are quite similar to the transitions with changing  $p$ . At  $g = 0$ , the firings are chaotic. As  $g$  is increased, the neurons exhibit transitions from spatiotemporal chaos to BS, then to APS, and finally to SS. Fig. 9 presents  $\sigma$  vs.  $g$  for different  $\tau$  at  $p = 0.1$ . For intermediate  $\tau$ ,  $\sigma$  passes through a minimum first and then increases and undergoes a maximum followed by a monotonous decrease as  $g$  is increased, representing the transitions from spatiotemporal chaos to BS, then to

APS, and finally to SS. For larger  $\tau$ , the value of  $g$  for the APS shifts to smaller. However, the occurrence of the APS with changing  $g$  only exists within a narrow interval of  $\tau = 15$ – $40$ , which means that the occurrence of the APS with changing coupling strength depends strongly on the value of time delay. This result shows that, the coupling strength can also induce complex synchronization transitions, especially, the APS in the neurons.

The above results show that the network topology and coupling strength can also lead to the complex synchronization transitions, in particular, to the APS state on the neuronal networks as the time delay does [51]. These novel phenomena provide us novel mechanisms for the synchronization transitions and the APS state in the neurons, and thus would help us more completely understand the roles of these parameters in the firing activity of the neurons. It is commonly assumed that time delays induce APS behavior by introducing phase slips, and hence zigzag fronts as well as alternative layer waves can appear that supplement the noise-induced excitations [51]. The  $p$  or  $g$ -induced APS behavior leads us to a conclusion that random connections or coupling strength has a function like phase slips and can help the neuron firings reach the APS behavior by adjusting phase slips. These results allow us to understand the origin of diversity of synchronous dynamical states observed in large neuronal networks, and may help us understand various synchronization phenomena among distant neurons and the information processing within the brain.

It is worth saying that the firing transitions on a network must be closely related to the network structure itself. The firing transitions observed in the present Newman–Watts network model ( $k = 2$ ) might not appear in other types of networks. For instance, the APS behavior was not observed in the firing transitions with rewiring probability  $p$  in the Watts–Strogatz small-world network model based on the Rulkov map ( $k = 4$ ) [51]. This qualitative difference may be a consequence of different initial connectivities of neurons and different network topologies for the Watts–Strogatz and the presently used small-world network.

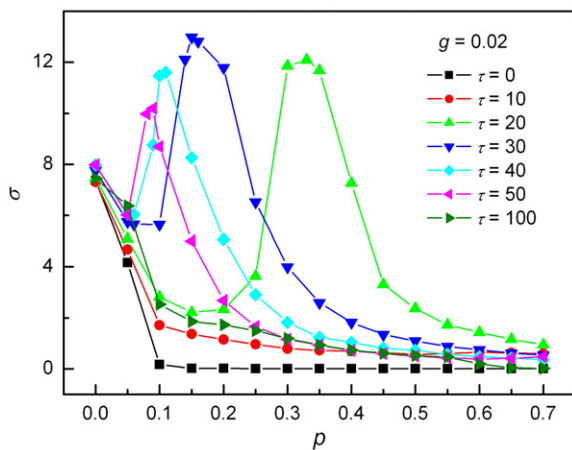


**Fig. 7.** Dependence of  $\sigma$  on  $p$  for different  $\tau$  at  $g = 0.02$ . For intermediate  $\tau$  values ( $20 \leq \tau \leq 50$ ),  $\sigma$  passes first through a minimum and then through a maximum, and finally decreases monotonously with increasing  $p$ , indicating transitions from spatiotemporal chaos to BS, then to APS, and finally to SS. But for  $\tau$  values outside the range, e.g.,  $\tau = 10$  or  $\tau = 100$ ,  $\sigma$  decreases monotonously with increasing  $p$ , indicating that there is no APS state and the firings change directly from spatiotemporal chaos to BS at  $\tau = 10$  or to SS at  $\tau = 100$ .

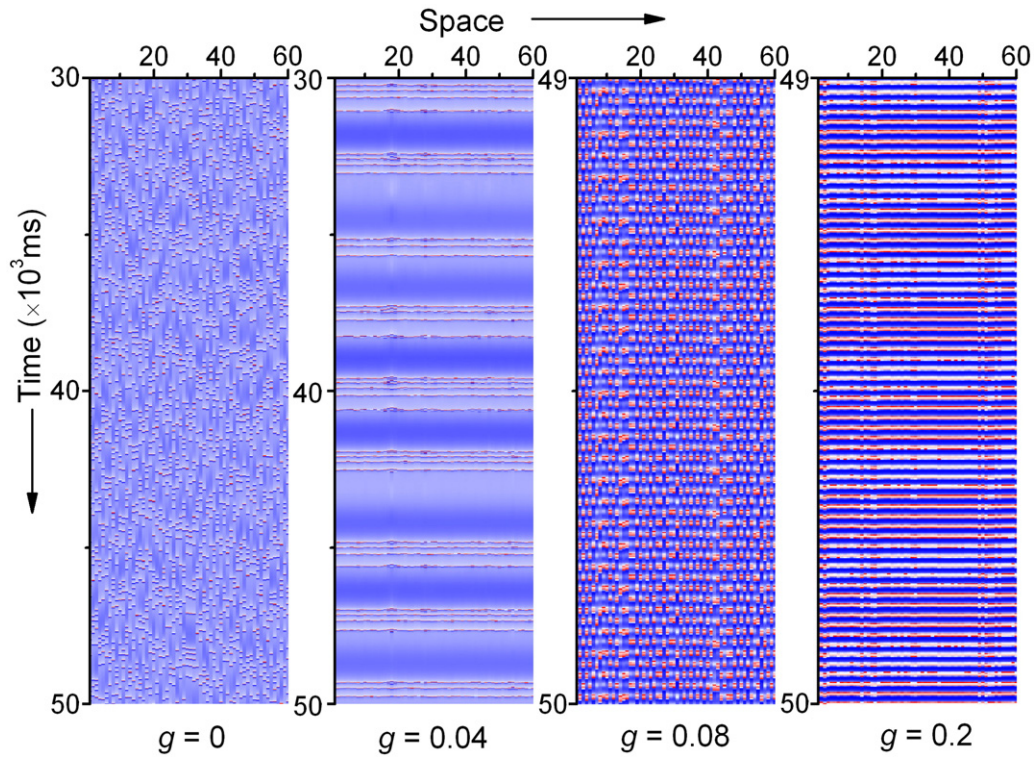


**Fig. 8.** Space–time plot of membrane potentials of the neurons for  $g = 0, 0.04, 0.08$ , and  $0.2$  at  $p = 0.1$  and  $\tau = 15$ . As  $g$  is increased, there are transitions from spatiotemporal chaos to BS, then to APS, and finally to SS.

#### 4. Conclusion

We have investigated the effects of time delay  $\tau$ , topological randomness  $p$ , and coupling strength  $g$  on synchronization transitions in chaotic MHH neurons on random networks. We found that the neurons exhibit transitions from BS to APS and finally to SS as  $\tau$  is increased. With increasing  $p$  or  $g$ , there are transitions from spatiotemporal chaos to BS, then to APS, and finally to SS. However, the APS with changing  $p$  or  $g$  only occurs within a narrow interval of  $\tau$  values. For  $\tau$  values outside this range, the APS behavior does not appear and the firings change directly from spatiotemporal chaos to BS or SS at small or large  $\tau$ . This shows that  $p$  or  $g$ -induced APS behavior depends strongly on the time delay, and the APS may appear

by the help of random connections or coupling strength at a time delay for which the APS does not occur originally.

Bursting and spiking are two types of firings in neurons, and BS and SS have already been found in real neural systems. Previous studies have shown that slow oscillations ( $f < 1$  Hz) observed in the electroencephalographic recordings of naturally sleeping humans and other mammals are considered to be the result of the BS of billions of neurons in the brain [58,59], while SS, which can be observed in motor cortical neurons [60,61] may facilitate the cortical organization of cognitive motor processes. These facts represent that various types of firing synchronizations have different effects in the information processing in the brain. Therefore, our findings may provide a new insight into the roles of the time delay, in particular, the topological randomness and coupling strength in firing synchronizations and their transitions in biological systems.

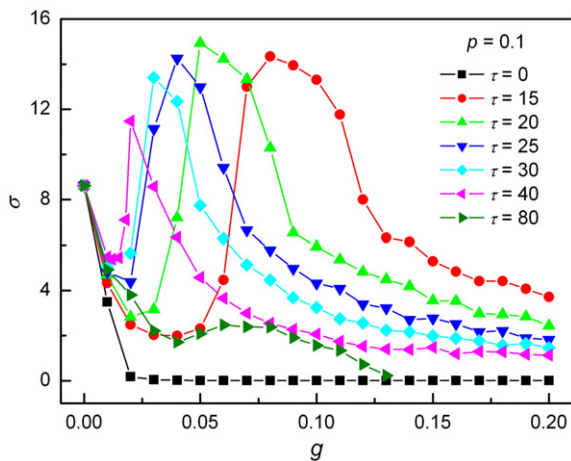


**Fig. 9.** Dependence of  $\sigma$  on  $g$  for different  $\tau$  at  $p = 0.1$ . The evolution of  $\sigma$  with increasing  $g$  is very similar to that with increasing  $p$  in Fig. 7, and the APS state only exists within a narrow range of  $\tau = 15$ –40.

#### Acknowledgment

The authors are thankful to the anonymous reviewer for helpful suggestions. This work was supported by the Natural Science Foundation of Shandong Province (Grant No. ZR2009AM016) and the Science Foundation of Ludong University (L20072805).

#### References

- [1] L. Gamaitoni, P. Hänggi, P. Jung, F. Marchesoni, Stochastic resonance, *Rev. Mod. Phys.* 70 (1998) 223–287.
- [2] J.J. Collins, C.C. Chow, A.C. Capela, T.T. Imhoff, Aperiodic stochastic resonance, *Phys. Rev. E* 54 (1996) 5575–5584.
- [3] A.S. Pikovsky, J. Kurths, Coherence resonance in a noise-driven excitable system, *Phys. Rev. Lett.* 78 (1997) 775–778.
- [4] S.G. Lee, A. Neiman, S. Kim, Coherence resonance in a Hodgkin–Huxley neuron, *Phys. Rev. E* 57 (1998) 3292–3297.
- [5] Y.B. Gong, Y.H. Hao, Y.H. Xie, X.G. Ma, C.L. Yang, Non-Gaussian noise optimized spiking activity of Hodgkin–Huxley neurons on random complex networks, *Biophys. Chem.* 144 (2009) 88–93.
- [6] J.A. White, J.T. Rubinstein, A.R. Kay, Channel noise in neurons, *Trends Neurosci.* 33 (2000) 131–137.



- [7] R.F. Fox, Y. Lu, Emergent collective behavior in large numbers of globally coupled independently stochastic ion channels, *Phys. Rev. E* 49 (1994) 3421–3431.
- [8] C.C. Chow, J.A. White, Spontaneous action potentials due to channel fluctuations, *Biophys. J.* 71 (1996) 3013–3021.
- [9] E. Schneidman, B. Freedman, I. Segev, Ion-channel stochasticity may be critical in determining the reliability and precision of spike timing, *Neuronal Comput.* 10 (1998) 1679–1703.
- [10] S.M. Bezrukov, I. Vodyanoy, Noise-induced enhancement of signal transduction across voltage-dependent ion channels, *Nature* 378 (1995) 362–364.
- [11] S.M. Bezrukov, I. Vodyanoy, Signal transduction across alamethicin ion channels in the presence of noise, *Biophys. J.* 73 (1997) 2456–2464.
- [12] G. Schmid, I. Goychuk, P. Hänggi, Optimal sizes of ion channel clusters, *EPL* 56 (2001) 22–28.
- [13] P. Hänggi, Stochastic resonance in biology, *ChemPhysChem* 3 (2002) 285–290.
- [14] M. Perc, A.K. Green, C.J. Dixon, M. Marhl, Establishing the stochastic nature of intracellular calcium oscillations from experimental data, *Biophys. Chem.* 132 (2008) 33–38.
- [15] M. Gosak, M. Marhl, M. Perc, Spatial coherence resonance in excitable biochemical media induced by internal noise, *Biophys. Chem.* 128 (2007) 210–214.
- [16] M.S. Wang, Z.H. Hou, H.W. Xin, Double-system size resonance for spiking activity of coupled Hodgkin–Huxley neurons, *ChemPhysChem* 5 (2004) 1602–1605.
- [17] Y.B. Gong, M.S. Wang, Z.H. Hou, H.W. Xin, Optimal spike coherence and synchronization on complex Hodgkin–Huxley neuron networks, *ChemPhysChem* 6 (2005) 1042–1047.
- [18] M. Perc, Effects of small-world connectivity on noise-induced temporal and spatial order in neural media, *Chaos, Solitons Fractals* 31 (2007) 280–291.
- [19] M. Ozer, M. Perc, M. Uzuntarla, Controlling the spontaneous spiking regularity via channel blocking on Newman–Watts networks of Hodgkin–Huxley neurons, *EPL* 86 (2009) 40008.
- [20] M. Ozer, M. Perc, M. Uzuntarla, Stochastic resonance on Newman–Watts networks of Hodgkin–Huxley neurons with local periodic driving, *Phys. Lett. A* 373 (2009) 964–968.
- [21] W. Singer, Synchronization of cortical activity and its putative role in information processing and learning, *Annu. Rev. Physiol.* 55 (1993) 349–374.
- [22] C.M. Gray, The temporal correlation hypothesis of visual feature integration: still alive and well, *Neuron* 24 (1999) 31–47.
- [23] P. Fries, D. Nikolić, W. Singer, The gamma cycle, *Trends Neurosci.* 30 (2007) 309–316.
- [24] R. Levy, W.D. Hutchison, A.M. Lozano, J.O. Dostrovsky, High-frequency synchronization of neuronal activity in the sub-thalamic nucleus of Parkinsonian patients with limb tremor, *J. Neurosci.* 20 (2000) 7766–7775.
- [25] F. Mormann, T. Kreuz, R.G. Andrzejak, P. David, K. Lehnertz, C.E. Elger, Epileptic seizures are preceded by a decrease in synchronization, *Epilepsy Res.* 53 (2003) 173–185.
- [26] M.I. Rabinovich, P. Varona, A.I. Selverston, H.D.I. Abarbanel, Dynamical principles of neuroscience, *Rev. Mod. Phys.* 78 (2006) 1213–1265.
- [27] A. Arenas, A. Diaz-Guilera, J. Kurths, Y. Moreno, C.S. Zhou, Synchronization in complex networks, *Phys. Rep.* 469 (2008) 93–153.
- [28] J.A.K. Suykens, G.V. Osipov, Introduction to focus issue: synchronization in complex networks, *Chaos* 18 (2008) 037101.
- [29] C.S. Zhou, J. Kurths, Noise-induced synchronization and coherence resonance of a Hodgkin–Huxley model of thermally sensitive neurons, *Chaos* 13 (2003) 401–409.
- [30] Q.Y. Wang, Q.S. Lu, G.R. Chen, Ordered bursting synchronization and complex wave propagation in a ring neuronal network, *Physica A* 374 (2007) 869–878.
- [31] B. Ibarz, H.J. Cao, M.A.F. Sanjuán, Bursting regimes in map-based neuron models coupled through fast threshold modulation, *Phys. Rev. E* 77 (2008) 051918.
- [32] Q.Y. Wang, Q.S. Lu, G.R. Chen, Subthreshold stimulus-aided temporal order and synchronization in a square lattice noisy neuronal network, *EPL* 77 (2007) 10004.
- [33] M. Perc, Optimal spatial synchronization on scale-free networks via noisy chemical synapses, *Biophys. Chem.* 141 (2009) 175–179.
- [34] S. Bahar, Burst-enhanced synchronization in an array of noisy coupled neurons, *Fluct. Noise Lett.* 4 (2004) L87–L96.
- [35] M. Yoshioka, Chaos synchronization in gap-junction-coupled neurons, *Phys. Rev. E* 71 (2005) 065203 R.
- [36] H. Hasegawa, Synchronizations in small-world networks of spiking neurons: diffusive versus sigmoid couplings, *Phys. Rev. E* 72 (2005) 056139.
- [37] Y.B. Gong, B. Xu, Q. Xu, C.L. Yang, T.Q. Ren, Z.H. Hou, H.W. Xin, Ordering spatiotemporal chaos in complex thermosensitive neuron networks, *Phys. Rev. E* 73 (2006) 046137.
- [38] D.Q. Wei, X.S. Luo, Ordering spatiotemporal chaos in discrete neural networks with small-world connections, *EPL* 78 (2007) 68004.
- [39] Y.H. Zheng, Q.S. Lu, Spatiotemporal patterns and chaotic burst synchronization in a small-world neuronal network, *Physica A* 387 (2008) 3719–3728.
- [40] Y. Shen, Z.H. Hou, H.W. Xin, Transition to burst synchronization in coupled neuron networks, *Phys. Rev. E* 77 (2008) 031920.
- [41] S. Postnova, K. Voigt, H.A. Braun, Neural synchronization at tonic-to-bursting transitions, *J. Biol. Phys.* 33 (2007) 129–143.
- [42] E.R. Kandel, J.H. Schwartz, T.M. Jessell, *Principles of Neural Science*, Elsevier, Amsterdam, 1991.
- [43] M. Dhamala, V.K. Jirsa, M.Z. Ding, Enhancement of neural synchrony by time delay, *Phys. Rev. Lett.* 92 (2004) 074104.
- [44] E. Rossoni, Y.H. Chen, M.Z. Ding, J.F. Feng, Stability of synchronous oscillations in a system of Hodgkin–Huxley neurons with delayed diffusive and pulsed coupling, *Phys. Rev. E* 71 (2005) 061904.
- [45] N. Burić, K. Todorović, N. Vasović, Synchronization of bursting neurons with delayed chemical synapses, *Phys. Rev. E* 78 (2008) 036211.
- [46] T.-W. Ko, G.B. Ermentrout, Effects of axonal time delay on synchronization and wave formation in sparsely coupled neuronal oscillators, *Phys. Rev. E* 76 (2007) 056206.
- [47] A. Roxin, N. Brunel, D. Hansel, Role of delays in shaping spatiotemporal dynamics of neuronal activity in large networks, *Phys. Rev. Lett.* 94 (2005) 238103.
- [48] Q.Y. Wang, M. Perc, Z.S. Duan, G.R. Chen, Delay-induced multiple stochastic resonances on scale-free neuronal networks, *Chaos* 19 (2009) 023112.
- [49] Q.Y. Wang, M. Perc, Z.S. Duan, G.R. Chen, Delay-enhanced coherence of spiral waves in noisy Hodgkin–Huxley neuronal networks, *Phys. Lett. A* 372 (2008) 5681–5687.
- [50] Q.Y. Wang, Q.S. Lu, G.R. Chen, Synchronization transition by synaptic delay in coupled fast spiking neurons, *Int. J. Bifurc. Chaos* 18 (2008) 1189–1198.
- [51] Q.Y. Wang, Z.S. Duan, M. Perc, G.R. Chen, Synchronization transitions on small-world neuronal networks: effects of information transmission delay and rewiring probability, *EPL* 83 (2008) 50008.
- [52] Q.Y. Wang, M. Perc, Z.S. Duan, G.R. Chen, Synchronization transitions on scale-free neuronal networks due to finite information transmission delays, *Phys. Rev. E* 80 (2009) 026206.
- [53] H.A. Braun, M.T. Huber, M. Dewald, K. Schäfer, K. Voigt, Computer simulations of neuronal signal transduction: the role of nonlinear dynamics and noise, *Int. J. Bifurc. Chaos* 8 (1998) 881–889.
- [54] H.A. Braun, H. Wissing, K. Schäfer, M.C. Hirsch, Oscillation and noise determine signal transduction in shark multimodal sensory cells, *Nature (Lond.)* 367 (1994) 270–273.
- [55] H.A. Braun, K. Schäfer, K. Voigt, R. Peters, F. Bretschneider, X. Pei, L. Wilkens, F. Moss, Low-dimensional dynamics in sensory biology 1: thermally sensitive electroreceptors of the catfish, *J. Comp. Neurosci.* 4 (1997) 335–347.
- [56] H.A. Braun, M. Dewald, K. Schäfer, K. Voigt, X. Pei, K. Dolan, F. Moss, Low-dimensional dynamics in sensory biology 2: facial cold receptors of the rat, *J. Comp. Neurosci.* 7 (1999) 17–32.
- [57] U. Feudel, A. Neiman, X. Pei, W. Wojtenek, H. Braun, M. Huber, F. Moss, Homoclinic bifurcation in a Hodgkin–Huxley model of thermally sensitive neurons, *Chaos* 10 (2000) 231–239.
- [58] M. Steriade, D.A. McCormick, T.J. Sejnowski, Thalamocortical oscillations in the sleeping and aroused brain, *Science* 262 (1993) 679–685.
- [59] F. Amzica, M. Steriade, Electrophysiological correlates of sleep delta waves, *Electroencephalogr. Clin. Neurophysiol.* 2 (1998) 69–83.
- [60] A. Riehle, S. Grün, M. Diesmann, A. Aertsen, Spike synchronization and rate modulation differentially involved in motor cortical function, *Science* 278 (1997) 1950–1953.
- [61] F. Grammont, A. Riehle, Spike synchronization and firing rate in a population of motor cortical neurons in relation to movement direction and reaction time, *Biol. Cybern.* 88 (2003) 360–373.